Journal of ELECTRONIC MATERIALS, Vol. 33, No. 3, 2004

Comparative Study of Electrically Conductive Thick Films with and without Glass

ZONGRONG LIU[1] and D.D.L. CHUNG[1,2]

1.—Composite Materials Research Laboratory, University at Buffalo, The State University of New York, Buffalo, NY 14260. 2.—E-mail: ddlchung@buffalo.edu

An air-fireable, glass-free, electrically conductive thick-film material (96.6% Ag, 1.38% Cu, 0.28% Al, 0.35% Ti, and 1.39% Sn by weight) and a conventional glass-containing, electrically conductive thick-film material (96.6% Ag and 3.4% glass frit by weight), both on alumina substrates, were studied by electrical, mechanical, thermal, and microscopic methods. The volume electrical resistivity of the glass-free thick film (2.5×10^{-6} Ω·cm, 30-μm thick) is lower than that of the glass-containing thick film (3.9×10^{-6} Ω·cm, 19-μm thick), with each film processed at its optimum firing temperature. The optimum firing temperature is 930°C and 850°C for glass-free and glass-containing thick films, respectively, as indicated by the criteria of low resistivity and high scratch resistance. The glass-free thick film has a higher scratch resistance than the glass-containing thick film, both fired at their respective optimum temperatures, suggesting that the former has higher bond strength to the alumina substrate. The formation process of the glass-free and glass-containing thick films is similar. The process involves solid-state diffusion of silver, which results in a silver network and grain boundaries. However, the sintering of silver particulates in the glass-containing thick film is enhanced by the viscous flow of glass.

Key words: Thick film, electrical conductor, air-fireable, glass-free

INTRODUCTION

Thick-film conductive materials have been investigated since the 1970s for use in interconnections in the electronic packaging industry. Precious metals, such as silver, gold, platinum, and palladium,[1–5] and other base metals, such as nickel, chromium, aluminum, and copper,[1,6–8] have been used as the main conductive components in thick-film materials. Most previous investigations used glass frit as the binder for bonding between the thick film and the substrate and for bonding among metal particles.[9,10] The shortcoming of using glass frit in thick-film conductive materials is related to (1) the low electrical conductivity of the glass and (2) the weak bond between the film and the substrate after heat treatment.

Recently, researchers began to develop glass-free compositions to improve the properties of thick films. The work can be roughly classified into two branches. One alternative to glass frit involves using a metal oxide as the binder. However, this results in relatively high electrical resistivity.[11] Another way to replace glass frit involves using an active metal component as the binder.[12] Thick films containing active metal components were generally fired in vacuum or in inert atmospheres. Consequently, the processing cost is high, and commercial use is limited.

Developing air-fireable, glass-free, electrically conductive metallic thick-film materials is the purpose of this research. A composite based on silver, containing titanium as the active component and exhibiting low electrical resistivity, was developed in previous work.[13,14] However, the advantages of air-fireable, glass-free thick films remain to be identified and elucidated. This work is a comparative study of thick film with and without glass. It addresses the sintering behavior by thermal analysis and by studying the effect of the peak processing temperature on the microstructure of the thick film. In addition, it characterizes the thick film after firing in terms of the electrical resistivity and scratch resistance.

(Received September 2, 2003; accepted September 3, 2003)

EXPERIMENTAL METHODS

The glass-free metal, thick-film composition used in this paper was 96.6% Ag, 1.38% Cu, 0.28% Al, 0.35% Ti, and 1.39% Sn (by weight).[14] The organic vehicle consisted of 60 wt.% ethyl cellulose and 40 wt.% di(ethylene glycol) butyl ether. The ether is a volatile solvent; ethyl cellulose is a solute dissolved in the ether for the purpose of increasing the viscosity and, hence, enhancing the suspension of the solid particles in the paste, in addition to improving the thermal stability of the paste.[15] The ratio of metal powders to the organic vehicle in the paste was 4:1. The glass-free paste in this paper consisted of three parts. Part A is the organic vehicle. Part B is a commercial paste, which is used as the source of active metal components, such as titanium and aluminum. The silver particles in the commercial paste have a particle size ranging from 15 μm to 30 μm and a spherical shape.[12] Part C is fine silver particulates, which are irregularly shaped, with size ranging from 1.5 μm to 2.5 μm.

The glass-containing thick film contained 96.6 wt.% Ag and 3.4 wt.% glass frit. Only fine silver particulates, which were the same as those in the glass-free paste (i.e., 1.5–2.5 μm), were used in this composition. The glass frit was supplied by SEM-COM Company. Inc. (Toledo, OH). The glass frit consists of silicon dioxide (<70 wt.%), boron oxide (<20 wt.%), and aluminum oxide (<10 wt.%). The weight ratio of the functional phases to the organic vehicle in the glass-containing paste was 3:1.

The standard, commercial alumina substrate (96% Al_2O_3, 50.8 mm × 50.8 mm × 0.6 mm) was used. The pastes were applied on alumina substrates manually. Firing of both glass-free and glass-containing films were conducted in air after the film had been allowed to dry in air at room temperature.

The firing of the glass-free thick-film material was conducted at 400°C, 450°C, 600°C, 750°C, 850°C, 900°C, or 930°C for 60 min, all with a heating rate of 15°C/min and a cooling rate of 40°C/min. All the samples were fired after they had been allowed to dry in air for 2 days.

The glass-containing thick-film samples were heated to 125°C for 15 min first with a heating rate of 50°C/min, followed by heating from 125°C to 400°C, 450°C, 600°C, 750°C, 850°C, 900°C, or 930°C at a heating rate of 50°C/min, holding at the maximum temperature for 60 min, and then cooling at a rate of 40°C/min. All the samples were fired 10 min after printing, i.e., 10 min of drying in air.

The surface morphology of the thick films after air firing was examined under a scanning electron microscope (SEM). Energy-dispersive x-ray spectroscopy was conducted using the SEM to analyze the elemental composition in selected regions of the microstructure.

The direct-current volume electrical resistivity of the thick films after firing was measured using the four-probe method. It was calculated from the measured resistance and thickness; both quantities were measured for each specimen. The film thickness was measured using an optical microscope. For measuring the resistance, four electrical contacts were made by soldering (tin-lead solder). The outer (current) probes were 48.5 mm apart; the inner (voltage) probes were 41.5 mm apart. Five specimens were tested for each combination of composition and peak-firing temperature.

Scratch testing of the thick films, as described in Ref. 12, was conducted using a 502 shear/scratch tester, which was manufactured by Teledyne Taber (North Tonawanda, NY). The specimen was mounted on a horizontally rotatable plate. A diamond scratching tool in the shape of a cone was used. The tool was attached to a finely balanced scale beam calibrated in grams. The load was 500 g. The scratch width was measured by the SEM. In this work, the scratch was not deep enough to cause substrate exposure for both thick films fired at their respective optimum-peak temperatures. Nevertheless, the smaller the scratch width is, the higher the shear strength is, which relates to both the bond strength of the thick film to the substrate and the shear strength within the thick film. Three specimens with three scratches on each specimen were measured for each combination of composition and peak-firing temperature.

The alumina substrate was also cut into 2 mm × 2 mm pieces for thermal analysis. The thick-film paste was applied to the alumina substrate and dried at room temperature for 2 days. No firing was conducted prior to thermal analysis, which was performed to study the process of firing. Some samples were then put in alumina pans and covered by alumina lids for differential scanning calorimetry (DSC), which was conducted in air using a Perkin-Elmer Corp. (Norwalk, CT) DSC 7 system. The samples were heated to 725°C at a heating rate of 15°C/min. In addition, DSC was conducted for the ethyl cellulose powder, which was heated to 500°C at a heating rate of 15°C/min. A Perkin-Elmer Corp. TGA 7 system was used for thermogravimetric analysis (TGA) of selected samples (before firing), which were heated to 930°C at a heating rate of 15°C/min then held at 930°C for 60 min.

RESULTS

Electrical Resistivity and Thickness

Table I shows the film thickness, which is smaller for the glass-containing thick films than the glass-free thick films for the same peak-firing temperature. For the same composition, the thickness has a tendency to decrease with increasing peak-firing temperature. However, for the glass-free thick films, the thickness increases slightly when the peak-firing temperature is above 850°C. This is probably caused by the oxidation of the active metal components in the thick film at higher temperatures, as supported by TGA.

Table II shows the volume electrical resistivity of thick films with and without glass after firing in air

Table I. Thickness (μm) of Thick Films with and without Glass after Firing at Different Peak Temperatures

	Peak-Firing Temperature (°C)						
Composition	**400**	**450**	**600**	**750**	**850**	**900**	**930**
A	54 ± 8	52 ± 6	48 ± 7	31 ± 4	27 ± 3	29 ± 3	30 ± 2
B	33 ± 5	32 ± 4	29 ± 4	19 ± 2	19 ± 2	19 ± 3	18 ± 2

A: 96.6Ag-1.38Cu-0.28Al-0.35Ti-1.39Sn (without glass)
B: 96.6Ag-3.4 glass frit

Table II. Volume Resistivity of Thick Films with and without Glass after Firing at Different Peak Temperatures (10^{-6} Ω·cm)

	Peak-Firing Temperature (°C)						
Composition	**400**	**450**	**600**	**750**	**850**	**900**	**930**
A	45.2 ± 8.2	43.9 ± 8.5	35.4 ± 5.9	19.2 ± 3.3	9.2 ± 1.1	5.3 ± 0.6	2.5 ± 0.2
B	15.9 ± 2.9	15.2 ± 2.1	11.9 ± 1.5	4.1 ± 0.7	3.9 ± 0.3	3.7 ± 0.4	3.7 ± 0.3

A: 96.6Ag-1.38Cu-0.28Al-0.35Ti-1.39Sn (without glass)
B: 96.6Ag-3.4 glass frit

Table III. Sheet Resistivity of Thick Films with and without Glass after Firing at Different Peak Temperatures (mΩ/square)

	Peak-Firing Temperature (°C)						
Composition	**400**	**450**	**600**	**750**	**850**	**900**	**930**
A	8.4 ± 1.5	8.4 ± 1.6	7.3 ± 1.2	6.2 ± 1.1	3.4 ± 0.4	1.9 ± 0.2	0.8 ± 0.1
B	4.8 ± 0.9	4.7 ± 0.6	4.1 ± 0.5	2.2 ± 0.4	2.1 ± 0.2	1.9 ± 0.2	2.0 ± 0.2

A: 96.6Ag-1.38Cu-0.28Al-0.35Ti-1.39Sn (without glass)
B: 96.6Ag-3.4 glass frit

at different temperatures. The resistivity decreases with increasing peak-firing temperature for both compositions. Table III shows the sheet resistivity, which is the volume resistivity divided by the thickness. The sheet resistivity of the glass-free thick film (composition A) is much less than that of the glass-containing thick film (composition B). This is because of the lower volume resistivity (Table II) and the larger thickness (Table I) of composition A.

The volume resistivity of the glass-containing thick film (composition B in Table II) levels off when the peak-firing temperature is above 750°C. The lowest value, as obtained at the peak-firing temperature of 900°C, is 3.7×10^{-6} Ω·cm, which is close to the values for the same composition fired at 750°C and 850°C. This volume resistivity corresponds to a sheet resistivity of 1.9 mΩ per square, as shown in Table III. The softening point of the glass used is 700°C. The leveling off of the resistivity above 750°C suggests that the microstructure essentially does not change if the peak-firing temperature is above the softening point of the glass. This point is supported by microscopy.

The resistivity of the glass-free thick film (composition A in Table II) decreases significantly with increasing peak-firing temperature. The lowest volume resistivity occurs at the highest peak-firing temperature of 930°C, i.e., 2.5×10^{-6} Ω·cm (sheet resistivity = 0.8 mΩ per square).

Table IV. The Scratch Width (μm) of Thick Films with and without Glass after Firing at Different Peak Temperatures and Scratch Testing at a Load of 500 g

	Peak-Firing Temperature (°C)			
Composition	**750**	**850**	**900**	**930**
A	276 ± 96	320 ± 105	110 ± 13	75 ± 8
B	137 ± 10	93 ± 9	90 ± 10	92 ± 7

A: 96.6Ag-1.38Cu-0.28Al-0.35Ti-1.39 Sn (without glass)
B: 96.6Ag-3.4 glass frit

The resistivity is 1.6×10^{-6} Ω·cm for pure silver.[16] The lowest resistivity of the glass-free thick film (2.5×10^{-6} Ω·cm) is higher than, but close to, that of pure silver.

Scratch Resistance

Table IV shows the scratch width of thick films with and without glass after firing at different peak temperatures. For the glass-free thick films, the width decreases sharply with increasing peak-firing

temperature. The narrowest width is 75 ± 8 μm, as obtained for a peak-firing temperature of 930°C. This means that the scratch resistance increases with increasing peak-firing temperature. Hence, the recommended peak-firing temperature for the glass-free thick film is 930°C, as shown by both high scratch resistance (Table IV) and low resistivity (Tables II and III).

There is no change in scratch width for the glass-containing thick films when the peak-firing temperature is above 850°C. Moreover, the resistivity leveled-off to a low value after firing at 850°C (Tables II and III). Hence, a peak-firing temperature of 850°C is recommended for the glass-containing thick film. This point is further supported by microstructural examination and thermal analysis. The scratch width of the thick film after firing at 850°C is greater than that of the glass-free thick film fired at 930°C. This suggests that the bond strength is higher for the glass-free thick film than the glass-containing thick film when they are fired at their respective optimum temperatures.

Figure 1a and b shows typical photographs of the scratched glass-free thick films after firing at 850°C and 930°C, respectively. Corresponding photographs of the scratched glass-containing thick films are shown in Fig. 1c and d, respectively. The alumina substrate was completely exposed after scratching of the glass-free thick film after firing at 850°C, as shown in Fig. 1a. The scratch has an irregular shape. Weakness within the film and poor bonding between the film and the substrate are the causes of the poor scratch resistance. Smoothness and a regular outline were observed for the scratches in the glass-free thick films after firing at 900°C (not shown here) and 930°C (shown in Fig. 1b). No debonding or chipping was observed in the scratched glass-free thick film after firing at 930°C.

Sintering Process

Thermal Analysis

A DSC thermogram of the glass-free thick film on the alumina substrate is shown in Fig. 2a. The sample was heated to 725°C at a rate of 15°C/min. No peak was observed for the melting of tin (melting point = 232°C) because of the low content of tin in the thick film. For the same reason, no peak corresponding to the melting of aluminum (melting

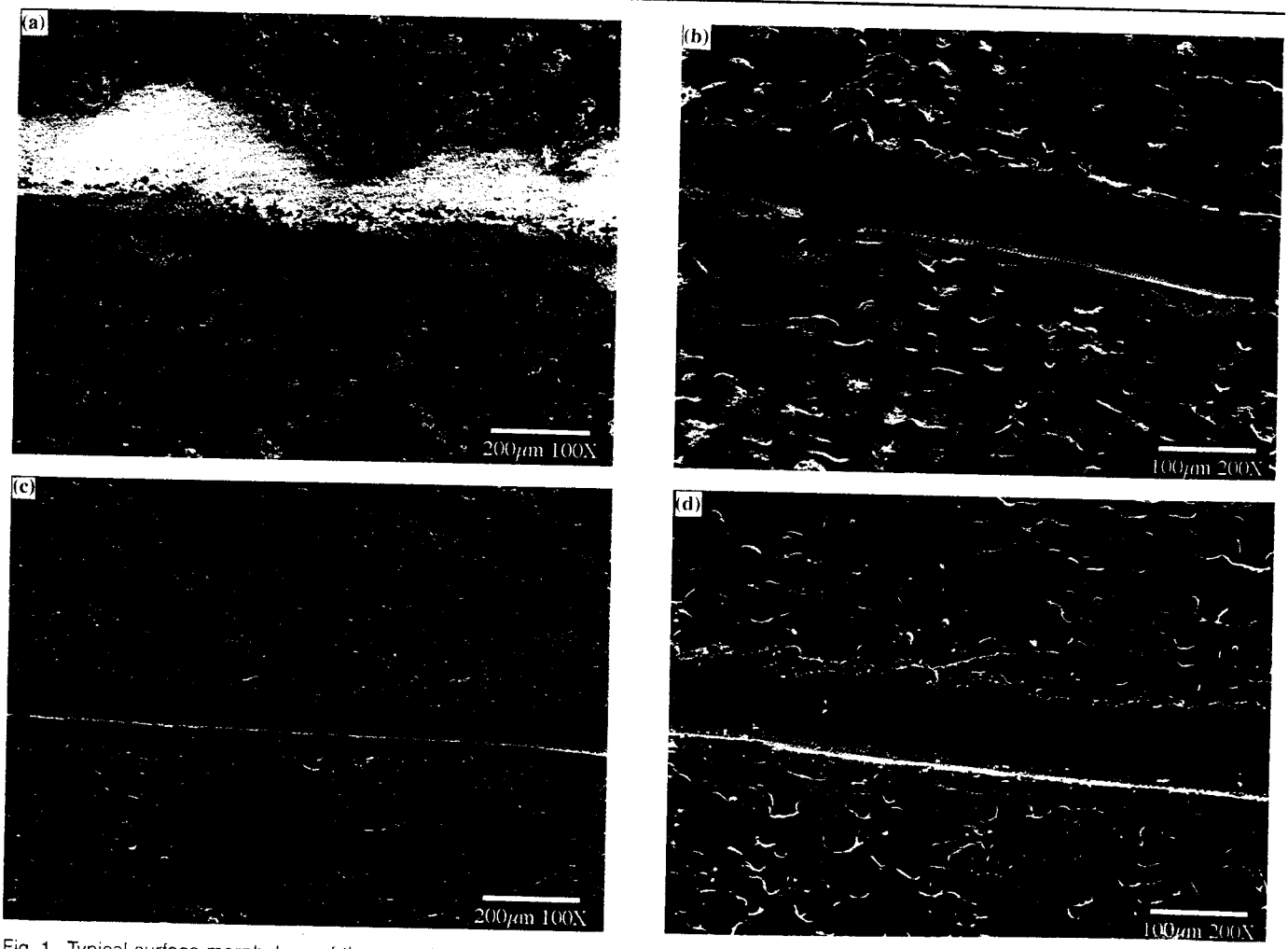

Fig. 1. Typical surface morphology of the scratched thick films: the glass-free thick films after firing at (a) 850°C and (b) 930°C and the glass-containing thick films after firing at (c) 850°C and (d) 930°C.

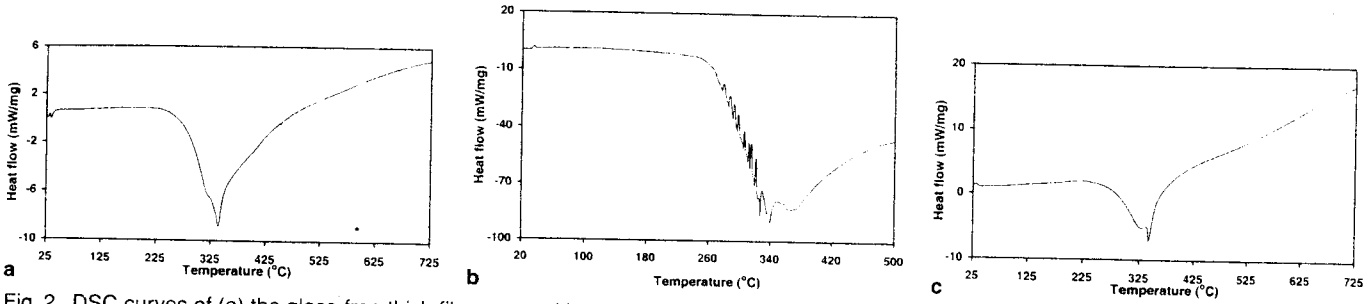

Fig. 2. DSC curves of (a) the glass-free thick-film composition, (b) ethyl cellulose, and (c) the glass-containing thick-film composition.

point = 660°C) was observed. An exothermic peak observed at an onset temperature of 258°C and a peak temperature of 340°C corresponds to the burn out of the ethyl cellulose component in the thick film. This interpretation is supported by DSC analysis of ethyl cellulose by itself, as shown in Fig. 2b. The thermogram at temperatures just below 340°C in Fig. 2b is not as smooth as that in Fig. 2a. This phenomenon is probably caused by the oxidation, pyrolysis, and volatilization of ethyl cellulose. The absence of this phenomenon in Fig. 2a may be due to the low content of ethyl cellulose in the thick film. The exothermic peak in Fig. 2b has an onset temperature of 258°C, as in Fig. 2a. This indicates that burn out of the ethyl cellulose in the thick film is not delayed by the presence of metal components.

Figure 2c is the DSC curve of the glass-containing thick film on the alumina substrate. The shape of the curve is similar to that in Fig. 2a. The viscous flow of the glass does not affect the shape of the DSC curve. The exothermic peak in Fig. 2c has an onset temperature of 258°C and a peak temperature of 342°C. This indicates that the burn out of the ethyl cellulose in the glass-containing thick film is not delayed by the presence of the glass. However, the peak temperatures in Fig. 2a (340°C) and Fig. 2c (342°C) are lower than that in Fig. 2b (372°C). The complete burn out of ethyl cellulose may occur at lower temperatures when the ethyl cellulose is present with solid components.

The TGA results in Fig. 3a and b show that most of the weight loss occurs below 300°C because of the

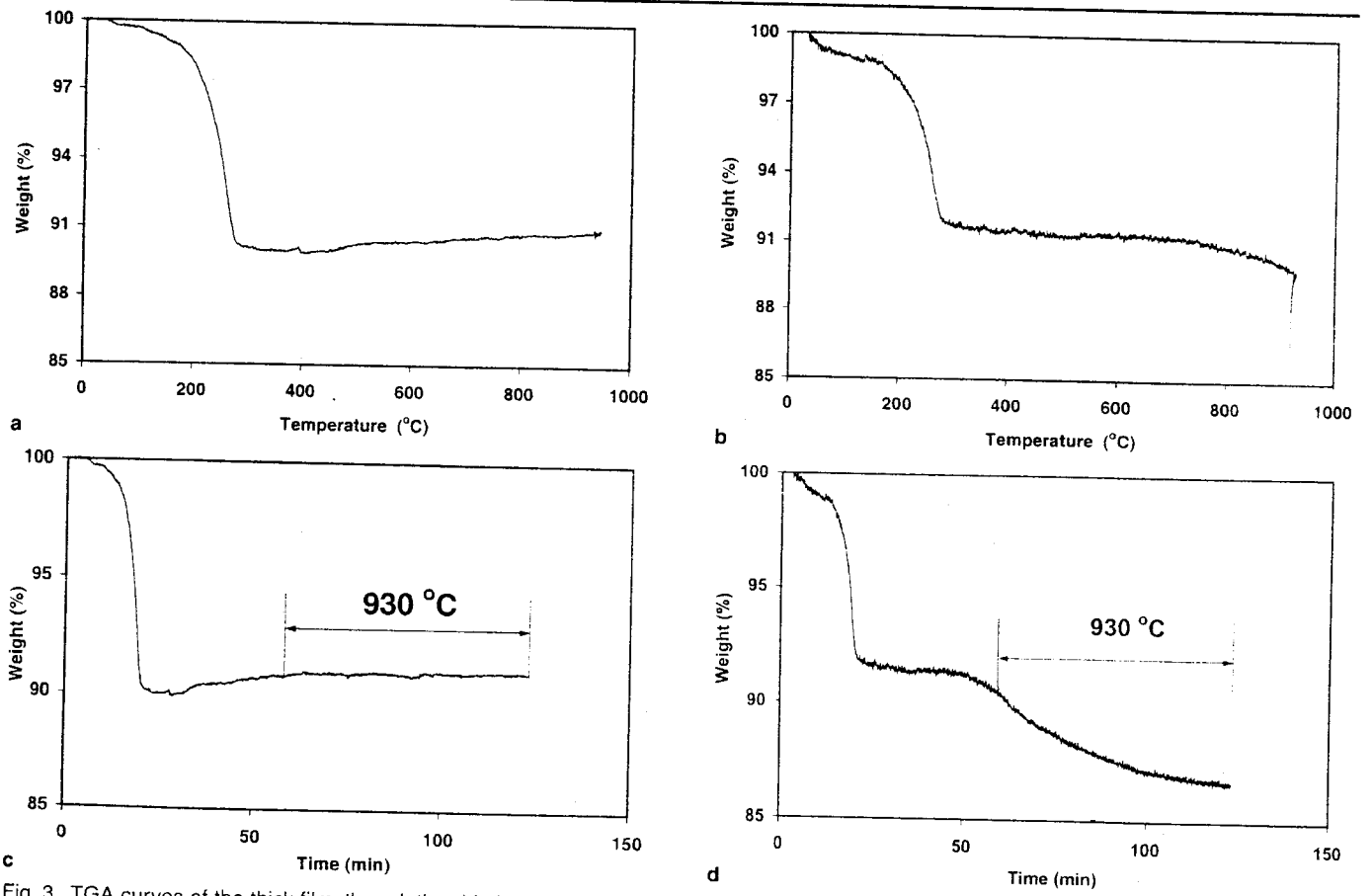

Fig. 3. TGA curves of the thick film: the relationship between the weight of the thick film and the temperature for the thick films (a) without and (b) with glass and the relationship between the weight of the thick film and the time for the thick films (c) without and (d) with glass.

burn out of the vehicle for both thick films with and without glass. Above 300°C, the glass-free thick film (Fig. 3a) gains weight slightly as the temperature increases up to 930°C probably because of the oxidation of the metal components in the thick film. In contrast, the glass-containing thick film (Fig. 3b) continuously loses weight as the temperature is increased from 300°C to 930°C. This is caused by the partial evaporation of the thick film, presumably caused by the evaporation of the glass. At 950°C, essentially the entire thick film disappeared because of extensive evaporation, as observed visually. Figure 3c and d shows the corresponding relationship of weight loss and heating time for the thick films without and with glass, respectively. The plots as a function of time show that the glass-free thick film gains weight slightly, and the glass-containing thick film continuously loses weight when the temperature is above 300°C; this extent of heating corresponds to a heating time of 20 min, as shown in Fig. 3c and d.

The glass-containing thick film has poor thermal stability at 930°C (Fig. 3d). This may also be the reason why most commercial, glass-containing thick-film pastes are recommended for firing at their peak-firing temperatures for no more than 30 min.

Microscopy

Silver particulates of 1.5–2.5 μm in size were used in both glass-free and glass-containing thick-film pastes. Figure 4 shows the silver particulates by themselves (i.e., not as a part of a thick film). Aggregation of the fine silver particulates occurs.

Figure 5a–d shows the typical surface morphology of the glass-free thick films after firing at 400°C, 750°C, 850°C, and 930°C for 60 min, respectively. Figure 6a–c shows the typical SEM photographs of the glass-containing thick films after firing at 400°C, 450°C, and 750°C for 60 min, respectively.

Necking between adjacent, fine silver particulates begins to occur at 400°C for both thick films without and with glass, as shown in Figs. 5a and 6a, although neck formation in the glass-containing thick film is more extensive. Ethyl cellulose is mostly burnt out at temperatures below 400°C for both thick films, as shown by TGA.

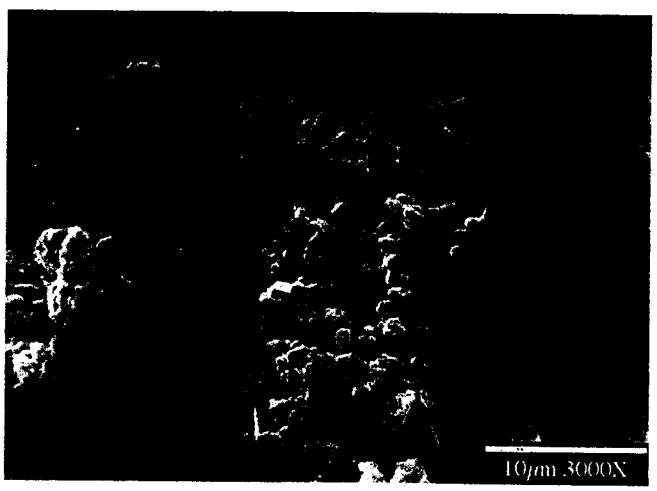

Fig. 4. Morphology of the fine silver particulates.

The necking becomes more extensive as the peak-firing temperature is increased for both thick films with and without glass. For the glass-free thick film, after firing at 750°C for 60 min, as shown in Fig. 5b, most of the fine silver particulates have lost their initial morphology (Fig. 4) because of the extensive network formation. However, there is still no evidence for the sintering of the coarse silver particles (labeled Ag in Fig. 5b), as the size and shape of these particles essentially do not change. After firing at 850°C for 60 min (Fig. 5c), the networking of the fine silver particulates is so extensive that the particulate network is replaced by patches. This suggests the occurrence of extensive solid-state flow in the fine silver particulates. In addition, most of the coarse silver particles begin to undergo diffusion, as suggested by their reduced size (<23 μm) compared to their original size (<30 μm). After firing at 900°C or 930°C (photo shown for 930°C only in Fig. 5d), essentially all of the fine silver particulates have been replaced by silver grains with well-defined grain boundaries between adjacent grains. In addition, diffusion has occurred in most of the coarse silver particles.

A common feature of glass-free thick films fired below 900°C is the presence of holes (labeled H in Fig. 5b and c and Fig. 6) and exposed substrate regions (labeled ES in Fig. 6) and the consequent local discontinuity in the film. Figure 6 shows the exposed substrate regions in the glass-free thick film fired at 900°C. The remnants of coarse silver particles after diffusion are labeled Ag in Fig. 6. After firing at 930°C (Fig. 5d), essentially all the silver particles, whether fine or coarse, have undergone extensive diffusion and relatively few pinholes were observed in the film. The scarcity of pinholes is consistent with the low volume resistivity of the film fired at 930°C (Table II). In addition, areas rich in copper, aluminum, tin, and titanium exist, as shown by x-ray spectroscopic elemental analysis in conjunction with the SEM (Fig. 5d). This is due to alloying among the metal elements. Details about the possible phases formed by the alloying needs further study.

Unlike the glass-free thick film, most of the fine silver particulates in the glass-containing thick film have lost their initial morphology at 450°C (Fig. 7b) because of the extensive network formation. Firing at 750°C (Fig. 7c) causes solid-state flow of silver particulates and the appearance of silver grain boundaries such that no part of the substrate is exposed. Essentially, no further microstructural change was observed in the glass-containing thick film when the peak-firing temperature is above 750°C (photograph not shown here). The dark spots in Fig. 7c, as shown

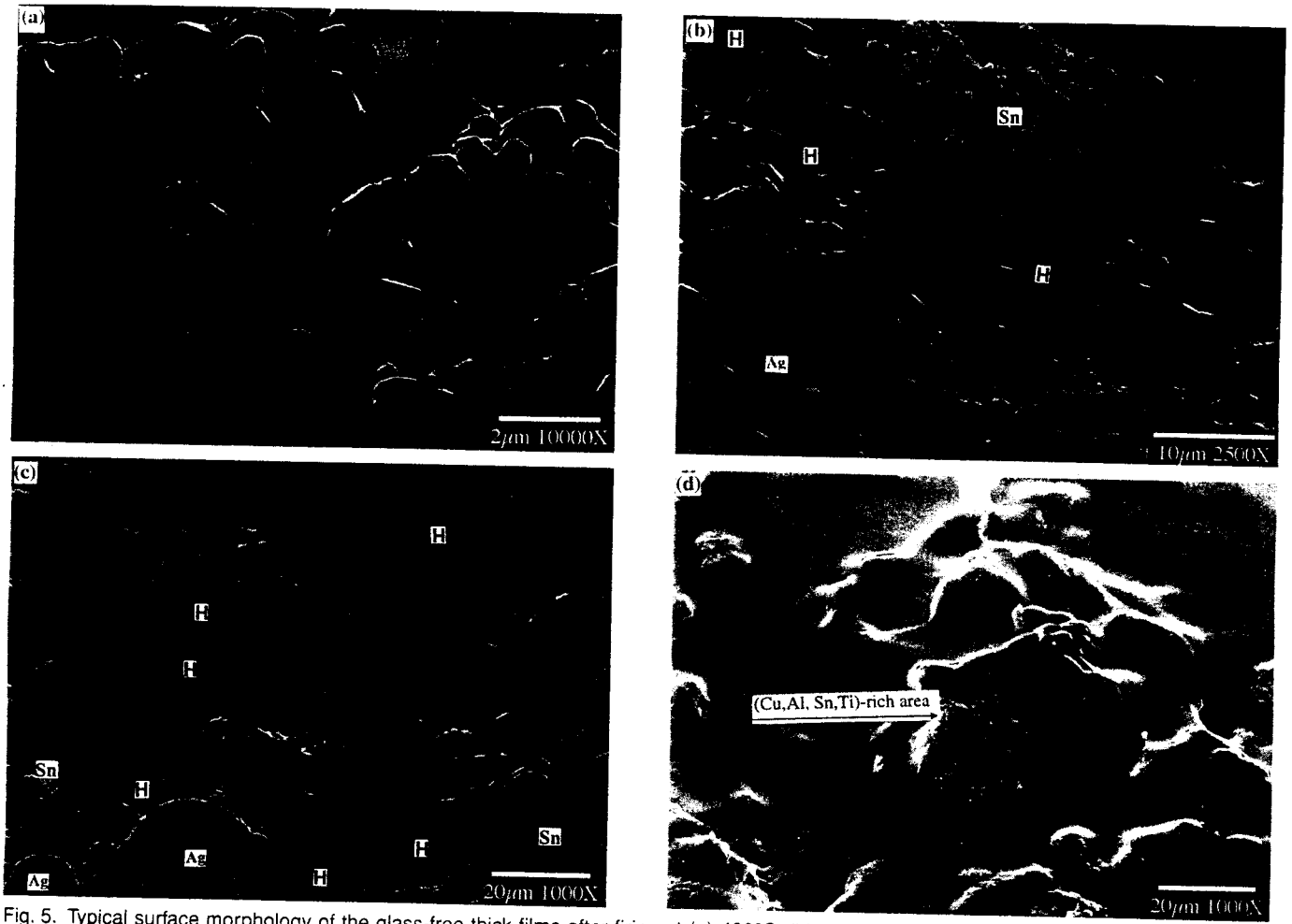

Fig. 5. Typical surface morphology of the glass-free thick films after firing at (a) 400°C, (b) 750°C, (c) 850°C, and (d) 930°C, respectively. H = hole; ES = exposed substrate.

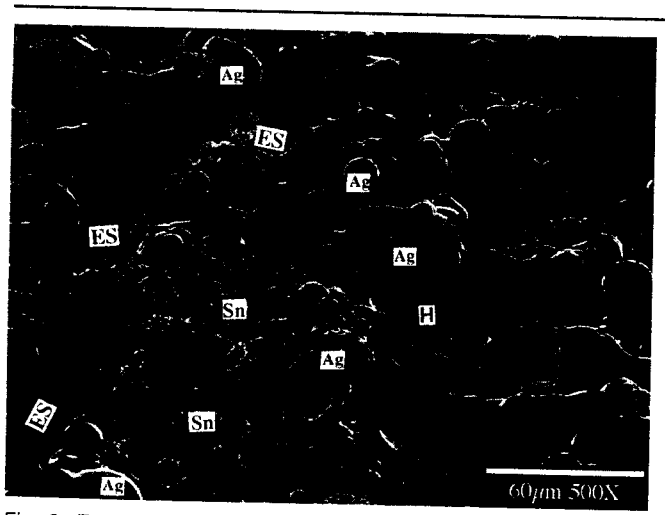

Fig. 6. Exposed substrate regions (labeled ES) in the glass-free thick film after firing at 900°C.

by arrows, are areas filled by molten glass during the firing.

Comparison of Fig. 5d and Fig. 7c indicates that a smoother thick-film surface can be obtained for the glass-free thick film fired at 930°C than the glass-containing thick film fired at 750°C.

DISCUSSION

According to the thermal analysis results and the microstructural examination, the process of the formation of thick films with and without glass can be described as follows.

In the initial stage of firing, the organic vehicle in the film evaporates and then burns out, resulting in holes and exposed substrate regions in the film. Thermal analysis shows that burn out of ethyl cellulose begins to occur around 258°C. Burn out of the vehicle involves the oxidation, pyrolysis, and volatilization of ethyl cellulose. Both the evaporation of the volatile di(ethylene glycol) butyl ether and burn out of ethyl cellulose result in the formation of holes and exposed substrate regions in the thick film.

Diffusion in the fine silver particulates with a size range of 1.5–2.5 μm begins to occur at 400°C, although extensive solid-state flow occurs only when the peak-firing temperature is higher than 850°C for the glass-free thick film. No melting occurs in the temperature range from 400°C to 930°C, according to high-temperature, differential-thermal analysis results, which constitute the subject of another paper and are not shown here. Increasing the peak-firing

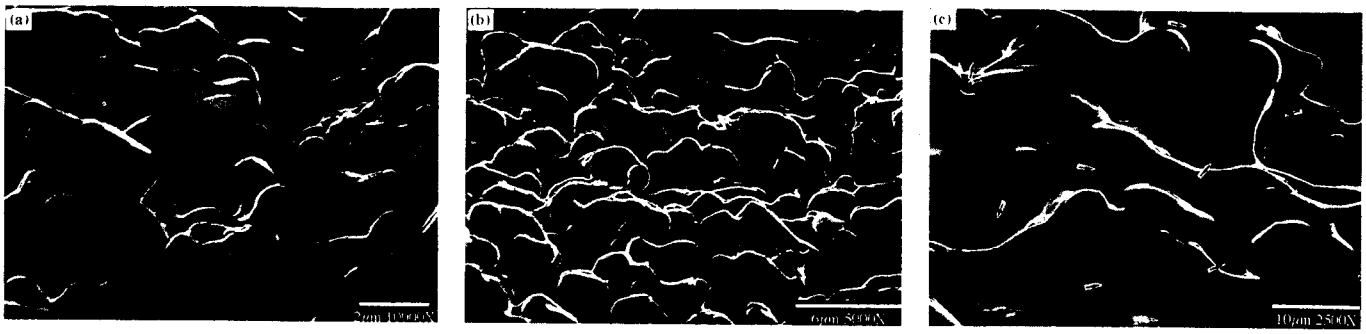

Fig. 7. Typical surface morphology of the glass-containing thick films after firing at (a) 400°C, (b) 450°C, and (c) 750°C, respectively. The arrows in (c) point at regions of molten glass.

temperature enhances the diffusion of silver and, consequently, facilitates the formation of the thick film.

The melting of tin, though not observed by DSC, may be helpful to the neck formation at low temperatures by allowing the diffusion of silver into the liquid tin. In addition, alloying, which occurs among different metal components during firing, and partial oxidation, which presumably occurs in the alloying element (copper, aluminum, and titanium) during firing, may help the affinity of silver with the alumina substrate. Further work is needed to confirm these hypotheses. A separate experiment (micrographs not shown here) showed that only a small number of silver particles remain on the substrate, and most of the film has disappeared after firing at 930°C in the case in which the thick film has no alloying element. Thus, the alloying elements are essential for thick-film formation. Furthermore, the alloying is expected to strengthen the thick film itself, thereby enhancing the scratch resistance.

Diffusion in the silver particulates of the glass-containing thick film is different from that of the glass-free thick film. Viscous flow of the glass facilitates the movement of the silver particulates. Such movement, along with diffusion in each silver particulate, helps network formation.

Based on the electrical resistivity and scratch testing results, the peak-firing temperatures at 930°C and 850°C are recommended for the glass-free thick film and glass-containing thick film, respectively. However, SEM characterization shows that the fine silver particulates completely flow at 850°C. Only the coarse silver particles, which are from Part B, need a peak-firing temperature as high as 930°C to flow completely. The ratio of the coarse silver particles and fine silver particulates is close to 1:2 in the glass-free thick film before firing. Hence, it is possible to reduce the optimum firing temperature to perhaps 850°C for the glass-free thick film if fine active metal particles are used in place of the coarse ones in Part B.

The electrical resistivity, the bond strength between the thick film and the substrate, and the cohesion within the thick film all depend on the hole density of the thick film. The lowest electrical resistivity and the highest scratch resistance attained in this work by firing the glass-free thick film at 930°C are associated with almost pinhole-free film quality. In addition, the use of active metal components instead of glass helps reduce the resistivity of the glass-free thick film. The higher scratch resistance of the glass-free thick film compared to the glass-containing thick film suggests higher bond strength, although it may be partly due to the higher strength within the alloyed thick film. In contrast, there is no alloying of the silver in the glass-containing thick film.

CONCLUSIONS

Based on the requirement of low resistivity and high scratch resistance, the recommended peak-firing temperatures for the glass-free and glass-containing thick films are 930°C and 850°C, respectively. The corresponding volume resistivity is 2.5×10^{-6} Ω·cm and 3.9×10^{-6} Ω·cm, respectively, for the glass-free and glass-containing thick films. The corresponding sheet resistivity is 0.8 mΩ per square and 2.1 mΩ per square, respectively. The glass-free thick film has a lower resistivity because of the use of the active metal binder instead of glass. The higher scratch resistance of the glass-free thick film suggests a higher bond strength, although it may be partly caused by the higher strength within the thick film caused by alloying among the metal components in the thick film. The thick-film formation process is similar for glass-free and glass-containing thick films, as both cases involve solid-state diffusion of silver. The diffusion results in network formation, followed by the appearance of silver grain boundaries. However, the glass in the glass-containing thick film facilitates networking because of its viscous flow.

REFERENCES

1. C.J.M. Lasance, H. Vinke, and H. Rosten, *IEEE Trans. Comp., Packaging, Manufacturing Technol.* 18, 1 (1995).
2. M. Novotny, *Precious Metals 1983 Proc.* (New York: Pergamon Press Inc., 1984), p. 69.
3. S.G. Yu, *Precious Metals 1987* (Allentown, PA: International Precious Metals Institute, 1987), p. 81.
4. R.R. Getty, B.E. Taylor, and C.R.S. Needs, *Solid State Technol.* 26, 163 (1983).
5. V.K. Nagesh and R.M. Fulrath, *Am. Ceram. Soc. Bull.* 58, 455 (1979).
6. S.J. Stein, C. Huang, and L. Cang, *Solid State Technol.* 24, 73 (1981).

7. T.R. Bloom, European patent EP 0558841 (Sept. 8, 1993).
8. F. Sirotti, M. Prudenziati, T. Manfredini, B. Giardullo, and W. Anzolin, *J. Mater. Sci.* 25, 4688 (1990).
9. S.B. Rane, T. Seth, G.J. Phatak, D.P. Amalnerkar, and M. Ghatpande, *J. Mater. Sci: Mater. Electron.* 15, 103 (2004).
10. A.G. Saunders, *Post Office Electr. Eng. J.* 73, 2 (1980).
11. S. Rane, V. Puri, and D. Amalnerkar, *J. Mater. Sci: Mater. Electron.* 11, 667 (2000).
12. M. Zhu and D.D.L. Chung, *J. Electron. Mater.* 23, 541 (1994).
13. Z. Liu and D.D.L. Chung, *J. Electron. Packaging* 123, 64 (2001).
14. Z. Liu and D.D.L. Chung, *J. Electron. Mater.* 30, 1458 (2001).
15. C.-K. Leong and D.D.L. Chung, *Carbon* 41, 2459 (2003).
16. G. Garter, *Principles of Physical and Chemical Metallurgy* (Metals Park, OH: ASM, 1979), p. 103.